


# ANALYTICAL INVESTIGATION ON THE CONDENSATION PERFORMANCE OF VERTICAL, TILTED AND HORIZONTAL SURFACES FOR PASSIVE WATER HARVESTING

Sahin GUNGOR\*, Department of Mechanical Engineering, Izmir Katip Celebi University, TURKEY, sahin.gungor@ikc.edu.tr  
( <https://orcid.org/0000-0003-1833-1484>)

Received: 10.02.2023, Accepted: 10.05.2023

Research Article

\*Corresponding author

DOI: 10.22531/muglajsci.1249821

## Abstract

Condensate harvesting is the phenomenon of obtaining water from water vapor in the humid air condensing on a surface. The idea is a passive technique with no additional energy consumption, yet condensation performance of a surface varies with many parameters. This study analytically investigates the condensation performance of the vertical, tilted, and horizontal water harvesting systems. First, viscous effects, inertia, and gravitational forces are examined in detail to express the evolution of boundary layer in condensation film. Then the condensation performance of each surface orientation and tilt angles are documented and compared for all flow conditions. Although vertical surfaces have higher condensate harvesting performance compared to the tilted and horizontal systems, the condensation rate is only about 2% lower up to 15° tilt angle. When the harvesting surface is tilted at 30°, the condensation rate of the laminar film decreases by 3.5%, while the reduction is 4.7% in wavy-turbulent film condensation. The results indicate that the change in condensation rate is more evident just after 45° tilt. Furthermore, 89° tilted surfaces experience 63.7% and 74.1% lower condensate harvesting in laminar and wavy-turbulent regimes, respectively. In addition, identical horizontal surfaces produce only one fifth condensation rate of a vertical system.

**Keywords:** Condensate harvesting, dew point, phase change, passive water harvesting, tilted surfaces.

## PASİF SU HASADI İÇİN DİKEY, EĞİMLİ VE YATAY YÜZEYLERİN YOĞUŞMA PERFORMANSININ ANALİTİK ARAŞTIRMASI

### Özet

Yoğuşma hasadı, bir yüzey üzerinde yoğunlaşan nemli havadaki su buharından su elde edilmesi olgusudur. Fikir, ek enerji tüketimi olmayan pasif bir tekniktir, ancak bir yüzeyin yoğuşma performansı birçok parametreye göre değişir. Bu çalışma, laminar, dalgali ve türbülanslı akış rejimleri altında dikey, eğimli ve yatay su toplama sistemlerinin yoğuşma performansını analitik olarak araştırmaktadır. İlk olarak, bir yoğuşma filminde sınır tabakasının gelişimini ifade etmek için viskoz etkiler, atalet ve yerçekimi kuvvetleri ayrıntılı olarak incelenir. Ardından, her yüzey yönünün ve eğim açılarının yoğuşma performansı belgelenir ve tüm akış koşulları için karşılaştırılır. Dikey yüzeyler eğimli ve yatay sistemlere göre daha yüksek kondens toplama performansına sahip olsa da, 15° eğim açısına kadar yoğuşma oranı sadece yaklaşık %2 daha düşüktür. Hasat yüzeyi 30° eğildiğinde, laminar filmin yoğuşma oranı %3,5 azalırken, dalgali-türbülanslı film yoğuşmasında azalma yaklaşık %4,7'dir. Sonuçlar, 45° eğim açılarından sonra değişimin daha belirgin olduğunu göstermektedir. Ayrıca, 89° eğimli yüzeyler, laminar ve dalgali-türbülanslı rejimlerde sırasıyla %63,7 ve %74,1 daha düşük yoğuşma hasadı yaşar. Ek olarak, aynı yatay yüzeyler, dikey bir sistemin yalnızca beşte biri yoğuşma oranı üretir.

**Anahtar Kelimeler:** Yoğuşma hasadı, çiy noktası, faz değişimi, pasif su hasadı, eğimli yüzeyler.

### Cite

Gungor, S., (2023). "Analytical investigations on the condensation performance of vertical, tilted and horizontal surfaces for passive water harvesting", *Mugla Journal of Science and Technology*, 9(1), 63-70.

## 1. Introduction

Condensate harvesting is a novel technique for fresh water harvesting from the humid atmosphere via condensation of water vapor in the air [1,2]. The harvesting strategy is physically related to the psychrometrics and heat transfer fields. Water vapor undergoes a phase change and becomes liquid once air is cooled to dew point temperature [3-5]. Condensate water can be collected with the help of a condensation surface positioned in various orientations and tilt angles. Furthermore, material properties of the condensation surface and interaction with water medium have evident impact on the harvesting performance [6, 7]. Literature classifies the atmospheric water harvesting strategies into three main subsections: dew condensation technologies, sorption systems, and active condensation technologies [8, 9]. Each technique is an alternative solution to obtain fresh water from different resources and avoid possible water shortages [10].

Condensation of water vapor from humid air is a passive harvesting strategy; therefore, no additional power supply is required to condense water vapor in the air medium. Poredos et al. investigated condensation performance of vertical flat plate systems in series [11]. The condensation surfaces are assumed to be isothermal over the entire plates, and the condensation regime is determined as laminar film [12]. They proposed a semi-empirical correlation to predict the condensation rate of the laminar condensation film on vertical flat plates. The proposed correlation has been compared with existing correlations and experimental data, and the results indicate that proposed correlation estimates the condensation mass flux in a range of  $\pm 12\%$  accuracy. Likewise, surfaces cooled by radiation below the dew point temperature of humid air yield-controlled condensation without additional energy consumption [13, 14]. Trosseille et al. [14] investigated controlled natural dew production and documented a radiative chamber for condensate harvesting. Evolution and formation of the dew is visualized, and they experimentally measured the quantity of radiative cooling power. In another study of the research team [15], they focused on how the water wetting properties affect the substrate emissivity and condensation performance. Emissivity of the samples are measured by an infrared camera and thermography mapping strategy. It is documented that dry substrate emissivity dominates the condensation performance at the beginning of the dew forming. On the other hand, Beysens et al. examined passive foil-based radiative condensers in dew collection point of view for various geographic locations [16]. This comprehensive study concluded that chemical quality of the harvested water is required to be well-known for operational performance. Furthermore, they documented the possibility of integrated water harvesting involving dew and rain together. In a broad perspective,

Tomaszkiewicz et al. [17] examined critical investigations on the dew physics [18-20] and reviewed the dew phenomenon in detail, and they expressed the condensate harvesting as a sustainable but non-conventional water resource.

The designs, materials and systems are evolving via technological improvements. Unfortunately, this evolution comes with some drawbacks, and access to fresh water may be a crucial problem in the near future. This study analytically uncovers the condensation performance of horizontal, vertical, and tilted surfaces under laminar, wavy and turbulent regimes in water harvesting point of view. The calculation steps, evolution of boundary layer thickness, and thermal phenomena among the dew surface and water vapor are documented in detail. Condensation performance of each investigated scenario is discussed in physical meaning, and then rates are nondimensionalized via the results of other orientations or flow regimes. The condensation performance of  $15^\circ$ ,  $30^\circ$ ,  $45^\circ$ , and  $75^\circ$  tilted surfaces are compared to horizontal and vertical dew systems for both laminar and wavy-turbulent film conditions. Furthermore, temperature based variation of the Prandtl number is reported and taken into account for the calculation of condensation performance.

## 2. Method and Models

Condensation performance of vertical, tilted, horizontal systems are considered under laminar, wavy and turbulent flow regimes to improve the accuracy of water harvesting. The flow is assumed as identical in the perpendicular direction; therefore, the governing equations are considered as two-dimensional. The conservation of mass, momentum, and energy equations of laminar regime investigations are given as follows [21, 22]:

$$\frac{\partial u}{\partial x} + \frac{\partial v}{\partial y} = 0 \quad (1)$$

$$\rho \left( u \frac{\partial u}{\partial x} + v \frac{\partial u}{\partial y} \right) = -\frac{\partial P}{\partial x} + \mu \nabla^2 u \quad (2)$$

$$\rho \left( u \frac{\partial v}{\partial x} + v \frac{\partial v}{\partial y} \right) = -\frac{\partial P}{\partial y} + \mu \nabla^2 v - \rho_l g \quad (3)$$

$$u \frac{\partial T}{\partial x} + v \frac{\partial T}{\partial y} = \alpha \nabla^2 T \quad (4)$$

where  $u$  is the  $x$ -component of the velocity vector,  $v$  denotes the  $y$ -component of the velocity vector,  $\rho_l$  is the density of water in liquid phase,  $P$  is the pressure,  $\mu$  represents the dynamic viscosity of the fluid,  $g$  is the gravitational acceleration,  $T$  denotes the temperature level, and  $\alpha$  represents the thermal diffusivity. On the other hand, the governing equations need to be revised for the turbulent regime investigations via  $u = \bar{u} + u'$ ,  $v = \bar{v} + v'$ ,  $P = \bar{P} + P'$ , and  $T = \bar{T} + T'$  terms containing average and fluctuation components [23, 24]. In this case, the momentum equations include  $(\partial/\partial x)(\bar{u}^2)$ ,  $(\partial/\partial y)(\bar{v}^2)$ ,  $(\partial/\partial x)(\bar{u}'v')$ , and  $(\partial/\partial y)(\bar{u}'v')$ , while the  $(\partial/\partial x)(\bar{u}'T')$

and  $(\partial/\partial y)(\overline{v'T'})$  terms are added into the energy equation [23]. Note that the dominant and negligible components of the partial derivatives vary with the orientation of the condensation surface.

In the vertical surfaces, pressure is only the function of longitudinal position, vertical pressure gradient in the liquid is identical with hydrostatic pressure of the vapor [22, 23].

$$\frac{\partial P}{\partial y} = \frac{dP}{dy} = -g\rho_v \quad (5)$$

Here,  $\rho_v$  represents the density of water vapor. The inertia effect in the momentum equations is negligible compared to the friction and sinking effects due to the slenderness of the structures (see Fig. 1). Therefore, the momentum equation (Eq. 3) simplifies as follows:

$$0 = -g\rho_v + g\rho_l + \mu \frac{d^2 v}{dx^2} \quad (6)$$

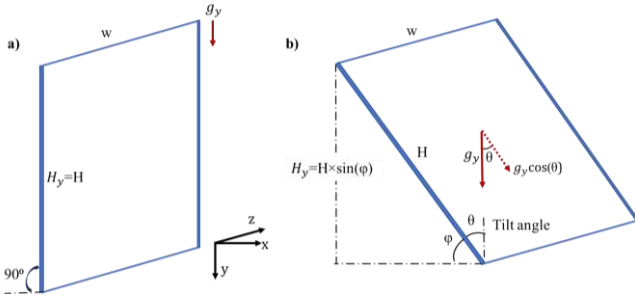


Figure 1. Vertical (a) and tilted surfaces (b) for the film condensation based water harvesting.

The  $g(\rho_l - \rho_v)$  term corresponds the sinking effect on the structure. Furthermore, velocity profile can be calculated analytically via integration of the following equation set [22, 23].

$$\mu \frac{d^2 v}{dx^2} = g(\rho_v - \rho_l) \quad (7)$$

$$\frac{dv}{dx} = \frac{g(\rho_v - \rho_l)}{\mu} x + C_1 \quad (8)$$

$$v = \frac{g(\rho_v - \rho_l)}{2\mu} x^2 + C_1 x + C_2 \quad (9)$$

In this equation set,  $C_1$  and  $C_2$  are the integration coefficients. We apply two boundary conditions to find the exact solution of the velocity profile. The first one is no-slip boundary condition ( $v = 0$  at  $x = 0$ ), and the latter is zero-shear at the liquid-vapor interface ( $dv/dx = 0$  when  $x = \delta$ ).

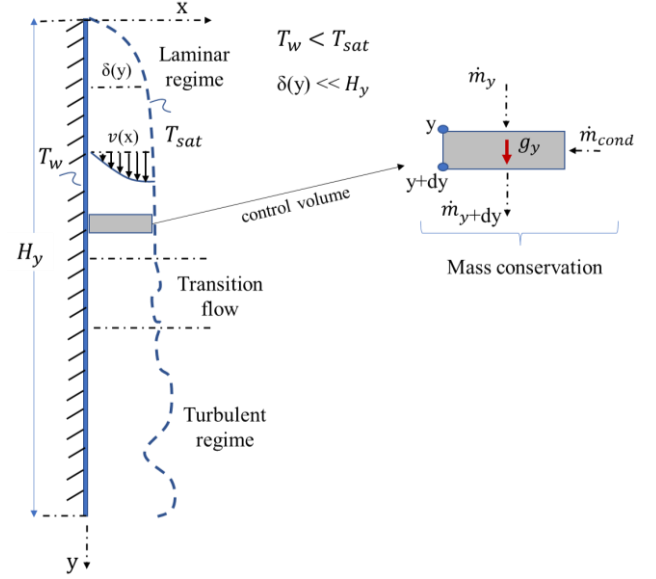


Figure 2. Flow regimes, velocity profile and film thickness on a representative condensation surface.

Note that  $\delta$  is the film thickness changing in the longitudinal direction  $\delta(y)$ . Once the no-slip and zero-shear boundary conditions are inserted in the main equation, we find  $C_2 = 0$  and  $C_1 = \frac{g\delta(\rho_l - \rho_v)}{\mu}$ . The velocity profile of the vertical liquid film is [11, 23]:

$$v(x, y) = \frac{g(\rho_l - \rho_v)}{2\mu} (2\delta x - x^2) \quad (10)$$

Velocity profile given in Eq. 10 present that the buoyancy effect is dominant in the film condensation problem. On the other hand, condensation mass flow rate is calculated by utilizing the conservation of mass:

$$\dot{m}_y + \dot{m}_{cond} - \dot{m}_{y+dy} = 0 \quad (11)$$

where  $\dot{m}_{cond}$  is the condensation mass flow rate entering the control volume. Figure 2 shows the selected control volume and mass flow rates in detail. Note that the condensation mass flow rate is equal the ratio between heat transfer through the selected control volume and latent heat due to the phase change ( $h_{fg}$ ). By expanding the  $\dot{m}_{y+dy}$  term via Taylor series and neglecting the high order terms, we obtain [22, 23]:

$$\dot{m}_y + \dot{m}_{cond} - (\dot{m}_y + \frac{d\dot{m}_y}{dy} dy) = 0 \quad (12)$$

$$\dot{m}_y = \int_0^\delta \rho_H v dx, \text{ per unit plate width} \quad (13)$$

$$\dot{m}_y = \frac{g\rho_l(\rho_l - \rho_v)}{3\mu} \delta^3 \quad (14)$$

$$\dot{m}_{cond} = \frac{Q}{h_{fg}} \quad (15)$$

in which the  $Q$  denotes the heat transfer rate and  $h_{fg}$  represents the latent heat of condensation phenomenon. Here the heat transfer rate is mainly due to the conduction mode as the inertia force is extremely small. Because the  $\delta(y) \ll H_y$ , we consider that the heat transfer exists only in one direction. Therefore, the rate

of heat transfer can be expressed by Fourier's law as follows [25, 26]:

$$q'' \approx -k \frac{dT}{dx} \approx -k \frac{T_{sat} - T_w}{\delta} \quad (16)$$

where  $q''$  is the heat flux absorbed by the wall,  $T_{sat}$  and  $T_w$  denote the saturation temperature and wall temperature, respectively. Combining the equations (12), (15) and (16), we obtain [22, 23]:

$$\mu \frac{d^2 v}{dx^2} = g(\rho_v - \rho_l) \quad (17)$$

$$\frac{dv}{dx} = \frac{g(\rho_v - \rho_l)}{\mu} x + C_1 \quad (18)$$

The film thickness in the longitudinal direction  $\delta(y)$  can be calculated after the integration of  $\delta = 0$  at  $y = 0$ :

$$\delta(y) = \left[ 4k\mu \frac{T_{sat} - T_w}{g\rho_l(\rho_l - \rho_v) h_{fg}} y \right]^{0.25} \quad (19)$$

On the other hand, augmented latent heat of  $h'_{fg}$  is recommended to use for transition (wavy) and turbulent regimes [21, 23]. This term contains both actual latent heat ( $h_{fg}$ ) and sensible heat contribution exists in case of  $T < T_{sat}$ . The augmented latent heat is calculated as follows:

$$h'_{fg} = h_{fg}(1 + 0.68 \text{Ja}) \quad (20)$$

$$\text{Ja} = C_p \frac{T_{sat} - T_w}{h_{fg}} \quad (21)$$

where Ja denotes the Jakob number corresponding the level of liquid film subcooling and  $C_p$  is the specific heat capacity at constant pressure. Note that it is required to use  $h'_{fg}$  for the film thickness if the flow regime is wavy or turbulent. At this point the Reynolds number of the flow should be checked via the given equation:

$$Re_y = \frac{4\dot{m}_H}{\mu} \quad (22)$$

In this flow regime calculation, both the mass flow rate and Reynolds number increase in the downstream direction (Fig. 2). Therefore, it is possible to see laminar flow regime in the vicinity of starting edge ( $y = 0$ ) while the flow may jump to wavy or turbulent flow regimes in parallel with the downward motion. The limits of the flow regime on vertical and tilted flat surfaces for the condensation physics are determined as follows [23]:

$$Re_y = \begin{cases} > 1800, \text{turbulent flow} \\ 30 - 1800, \text{transition (wavy)} \\ < 30, \text{laminar flow} \end{cases} \quad (23)$$

### 3. Results and Discussion

Regarding the physical meaning of boundary layer approach and flow regime limits, we analytically obtain the variation of film thickness by the help of slenderness assumption for the condensation surfaces. From thermal point of view, local heat transfer coefficient is calculated as [25, 27]:

$$h_y = \frac{q''}{\Delta T} = \frac{k}{\delta} \quad (24)$$

Combining the equations (19) and (22):

$$h_y = \left[ \frac{g\rho_l(\rho_l - \rho_v) h_{fg}}{4\mu y k^{-3} (T_{sat} - T_w)} \right]^{0.25} \quad (25)$$

Likewise, the overall heat transfer coefficient experienced by the laminar region is:

$$\bar{h} = \frac{1}{H_y} \int_0^H h_y dy \quad (26)$$

$$\bar{h} = \frac{4}{3} h_H \quad (27)$$

The average Nusselt number of the laminar film:

$$\bar{Nu} = \frac{\bar{h} H}{k} \quad (28)$$

$$\bar{Nu}_H = \frac{4}{3} \left[ \frac{g\rho_l(\rho_l - \rho_v) h_{fg}}{4\mu y k^{-3} (T_{sat} - T_w)} \right]^{0.25} \frac{H}{k} \quad (29)$$

$$\bar{Nu}_H = 0.9428 \left[ \frac{g\rho_l(\rho_l - \rho_v) h_{fg} H^3}{\mu k (T_{sat} - T_w)} \right]^{0.25} \quad (30)$$

On the other hand, determination of the average heat transfer coefficient in transition and turbulent regimes is more complicated and based on the experimental investigations. Following correlation presents the average heat transfer coefficient of wavy and turbulent regions [28]:

$$\bar{h} = k \left( \frac{g\rho_l^2}{\mu^2} \right)^{1/3} (Re_H^{-0.44} + 5.82) \times 10^{-6} Re_H^{0.8} Pr_H^{1/3} \quad (31)$$

$$\frac{\bar{h}}{k} \left( \frac{v_l^2}{g} \right)^{1/3} = (Re_H^{-0.44} + 5.82) \times 10^{-6} Re_H^{0.8} Pr_H^{1/3} \quad (32)$$

where  $\nu$  and  $Pr$  are the kinematic viscosity and Prandtl number, respectively. Likewise, Nusselt number of wavy or turbulent films can be calculated as follows:

$$\bar{Nu}_H = H_{wt} \left( \frac{g\rho_l^2}{\mu^2} \right)^{1/3} (Re_H^{-0.44} + 5.82) \times 10^{-6} Re_H^{0.8} Pr_H^{1/3} \quad (33)$$

Furthermore, Bejan [23] proposed a dimensionless group (B) for the driving parameter of film condensation problem. This phenomenon expresses the relation among the condensation rate, plate height and the temperature difference. The driving parameter of film condensation is given [23]:

$$B = \frac{4kH}{\mu h'_{fg}} (T_{sat} - T_w) \left( \frac{g}{v_l^2} \right)^{1/3} \quad (34)$$

$$B \approx 0.681Re_H^{4/3}, \text{ laminar regime} \quad (35)$$

$$B = Re_H(Re_H^{-0.44} + 5.82 \times 10^{-6}Re_H^{0.8}Pr_H^{1/3})^{-0.5}, \quad (36)$$

turbulent regime

Note that the film temperature approach is applied for thermophysical properties except the latent heat of phase-change ( $h'_{fg}$ ) and liquid phase density. Another critical issue is the sinking effect term as the density at the liquid phase is comparatively greater than the vapor one, e.g.,  $\rho_l \approx 1600\rho_v$  at 100°C [29]. Therefore, vapor phase density can be neglected in practical applications to simplify the correlations given above. On the other hand, Nusselt number correlation varies if the condensation surface is totally horizontal [30]:

$$\overline{Nu}_L = 1.079 \left[ \frac{g\rho_l(\rho_l - \rho_v) h'_{fg} L^3}{\mu k(T_{sat} - T_w)} \right]^{0.2} \quad L = H \quad (37)$$

In the calculation of vertical and tilted surfaces the most dominant parameter affecting the condensation rate and thermal performance is gravitational acceleration. The variation of Reynolds number for vertical and tilted surfaces experiencing film condensation are presented in Fig. 3 under laminar and wavy-turbulent flow conditions. Equation (22) indicates that the total mass flow rate of condensation film determines the Reynold number for each flow regime. Note that the total condensation rate per unit plate width varies with Nusselt number as follows:

$$\dot{m}'_H = \frac{k}{h'_{fg}} (T_{sat} - T_w) \overline{Nu}_H \quad (38)$$

The findings show that change in the total condensation rate of the wavy-turbulent regime film is much greater than the laminar film especially after 30° tilt angle. The condensation rate difference between the vertical plate ( $\theta = 0^\circ$ ) and 15° tilted surface is about 2% for both laminar and wavy-turbulent film regimes.

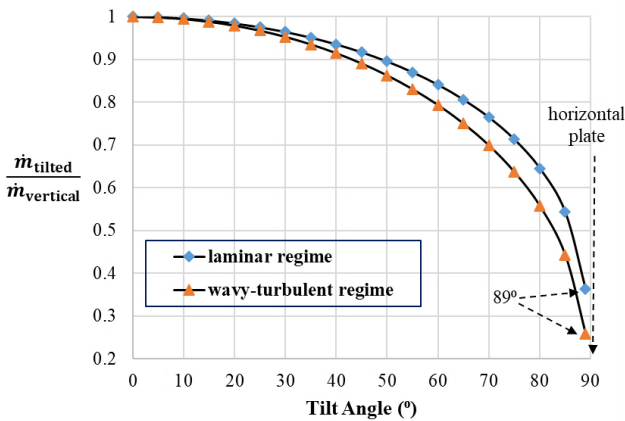


Figure 3. Condensation rate trend for vertical and tilted surfaces.

The rate of condensation film directly indicates the water harvesting performance, and tilt angle is the dominant parameter for these systems. When the surface is tilted at 30°, the condensation rate of the

laminar film decreases by 3.5%, while the reduction reaches 4.7% under wavy-turbulent regime. In the laminar film, the condensation rate is 8.3%, 15.9% and 28.7% smaller than the vertical plate when the tilt angles are 45°, 60° and 75°, respectively. Note that only 36.3% of the total condensation rate of vertical plate is produced by the tilted identical surface area when the angle with the horizontal axis is at 1° ( $\theta = 89^\circ$ ). On the other hand, total condensation rate of wavy-turbulent film decreases by 10.9%, 20.7% and 36.3% when the vertical plate is tilted at 45°, 60° and 75° angles, respectively. In the extreme case of  $\theta = 89^\circ$ , the tilted surface experiences only 25.9% condensation rate of the vertical plate scenario.

Condensate water flow splits from the center over the surface edges when the cooled surface is horizontal and condensation surface is upward. In this case, we utilize Eq. (37) to calculate the Nusselt number of horizontally located systems. Physical relation among the condensation performance of the vertical and horizontal surfaces under laminar regime conditions can be expressed as follows:

$$\dot{m}'_{ver} = 0.874 \dot{m}'_{hor} X^{0.05} \quad (39)$$

$$X = \frac{g\rho_l(\rho_l - \rho_v) h'_{fg} H^3}{\mu k(T_{sat} - T_w)} \quad (40)$$

where X is identical for the vertical and horizontal ( $H=L$ ) applications, yet the exponent of the vertical plate is 0.25 (Eq. 30) while the value is 0.2 (Eq. 37) for the horizontal laminar film condensation. The trend of condensation rate change in vertical and horizontal surfaces is given in Table 1.

Table 1. Film condensation performance of vertical and horizontal surfaces for water harvesting.

	Parameter group (X)							
	10 <sup>2</sup>	10 <sup>4</sup>	10 <sup>6</sup>	10 <sup>8</sup>	10 <sup>10</sup>	10 <sup>12</sup>	10 <sup>14</sup>	10 <sup>16</sup>
$\frac{\dot{m}'_{horizontal}}{\dot{m}'_{vertical}}$	0.901	0.724	0.574	0.456	0.362	0.362	0.228	0.181

Note that the size of the condensation surface is dominant parameter in the parameter group as the X varies with the third power of the surface dimension. The findings indicate that condensation performance of a horizontal surface is always lower than the identical vertical one. Furthermore, the condensation discrepancy increases in parallel with parameter group of X. Likewise, the condensation ratio of the horizontal and tilted surfaces under laminar film condensation regime is presented in Fig. 4. The results show that the change in condensation rate is more evident just after 45° tilt. The difference in condensation rate between the vertical and 75° tilted surfaces reaches up to 40.2% at the maximum parameter group level.

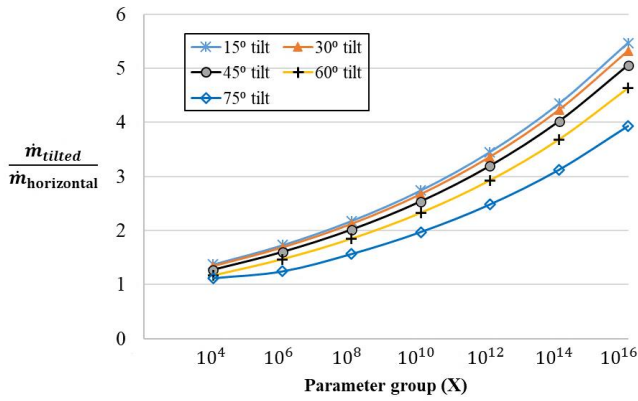


Figure 4. Laminar film condensation performance of tilted and horizontal surfaces for various parameter group levels.

As expected, the calculation steps and parameters are more complicated in the wavy and turbulent film condensation part. Gravitational acceleration in a vertical surface under wavy-turbulent regime conditions varies by one-third to the power, while the exponent of the horizontal plate is one-fifth. Furthermore, Prandtl number is an additional dimensionless parameter in turbulent films compared to the laminar film condensation problem. Therefore, main difference among the vertical and horizontal surfaces having wavy-turbulent films is not only the exponent of gravitational acceleration but also the Prandtl number at the given conditions.

Table 2. Wavy-turbulent regime film condensation performance of vertical and horizontal surfaces.

	Pr					
	0.5	1	2	5	10	20
$\frac{\dot{m}_{horizontal}}{\dot{m}_{vertical}}$	0.223	0.198	0.177	0.152	0.135	0.121

The condensation rates of horizontal and vertical flat surfaces are presented in Table 2 for various Prandtl numbers. The findings show that discrepancy among the vertical and horizontal systems increase with fluids having greater Prandtl number. In wavy-turbulent film systems, an identical horizontal surface can generate only 22.3% condensation performance of vertical one when the  $Pr = 0.5$ . The condensation ratio between the horizontal and vertical surfaces decreases from 19.8% to 17.7% for  $Pr = 1$  and  $Pr = 2$ , respectively. Furthermore, condensation performance of a vertical surface in wavy-turbulent regime is about 7.4 times higher than an identical horizontal one at  $Pr = 10$ . Table 1 and 2 also indicate that the discrepancy among the condensation rates of vertical, tilted and horizontal surfaces increases in wavy-turbulent regime systems. Figure 5 shows the trend of Prandtl numbers for water vapor and liquid water at distinct temperature levels [31, 32].

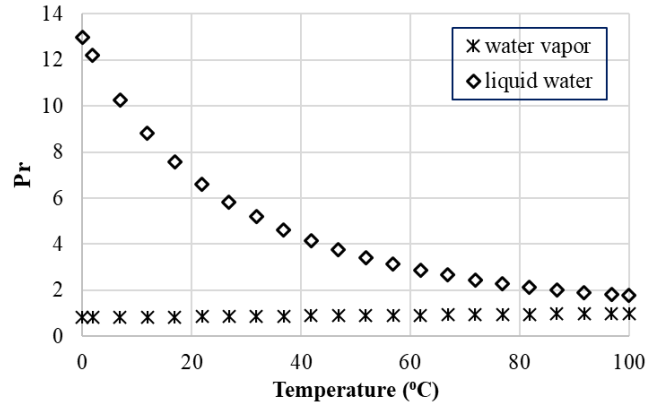


Figure 5. Prandtl number curves of water medium [27, 31].

Tilt angle is a dominant and key parameter affecting the condensation performance of water harvesting systems. Compared to the laminar film condensation, tilt angle has more impact on the condensation rate of wavy-turbulent systems especially at greater Prandtl numbers. The dimensionless condensation rates of horizontal and tilted systems are presented in Fig. 6 for  $Re_H > 30$  regime. The condensation discrepancy among the tilted surfaces is more evident in the wavy-turbulent film condensation. 75° tilted surface at  $Pr = 0.5$  generates almost triple condensation rate of a horizontal one, yet it corresponds only 64% condensation performance of a 15° tilted system. The results indicate almost linear relationship among the Prandtl number and tilted system condensation performance in wavy-turbulent flow regime. Furthermore, differences in the condensation rates highly increase just after 45° tilt angle. When the  $Pr = 2$ , condensation performance of a horizontal flat surface is only about 22.3% and 27.8% of the 60° and 75° tilted systems, respectively.

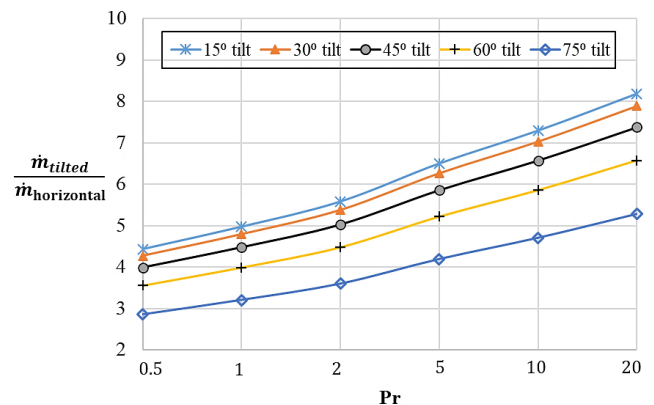


Figure 6. Comparison of tilted and horizontal surfaces under wavy-turbulent regime conditions.

#### 4. Conclusion

Condensate harvesting is basically the idea of obtaining water from water vapor in the humid air condensing on a surface. The condensation phenomenon enables passive water harvesting from the humid air, yet physical observations and experimental investigations on the condensation performance require advance infrastructure and equipment. Therefore, the analytical and theoretical ways seem more convenient for the flat surfaces. This study analytically uncovers the condensation performance of vertical, tilted and horizontal surfaces under laminar, wavy and turbulent flow regimes. The calculation strategies of boundary layer thickness, overall Nusselt number, and film condensation rate are physically discussed and expressed in detail for each flow condition. Furthermore, the condensation performance of tilted surfaces is documented at various tilt angles and compared to vertical and horizontal systems for laminar, wavy and turbulent flow regimes. The results indicate that condensation performance of the laminar film is always lower than the wavy-turbulent flow systems regardless of the surface orientation. The rate of condensation film directly presents the water harvesting performance, and tilt angle dominates the condensation rate for each orientation. When the harvesting surface is tilted at  $30^\circ$ , the condensation rate of the wavy-turbulent film decreases by 4.7%, while the reduction is about 3.5% in laminar film condensation. Moreover, condensation performance of the  $45^\circ$ ,  $60^\circ$  and  $75^\circ$  tilted surfaces decreases by 8.3%, 15.9% and 28.7% under laminar flow regime, while the performance losses reach up to 10.9%, 20.7% and 36.3% in wavy-turbulent film condensation at identical tilt angles. The wavy-turbulent regime extreme case of  $\theta = 89^\circ$  experiences only 25.9% condensation rate of the vertical plate scenario, while an identical horizontal surface produces less than 18% condensation when the  $Pr \geq 2$ . The proposed calculation steps are applicable to any flat surface based water harvesting system with minor geometrical and thermophysical modifications.

#### 5. Acknowledgment

The Author would like to express his deepest appreciation to the anonymous Reviewers and Editorial team for their contribution on the work.

#### 6. References

- [1] Liu, X., Beysens, D. and Bourouina, T., "Water harvesting from air: Current passive approaches and outlook", *ACS Materials Letters*, 4, 5, 1003-1024, 2022.
- [2] Tu, Y.D., Wang, R.Z., Zhang, Y.N. and Wang, J.Y., "Progress and expectation of atmospheric water harvesting", *Joule*, 2, 1452-1475, 2018.
- [3] Zhuang, S., Qi, H., Wang, X., Li, X., Liu, K., Liu, J. and Zhang, H., "Advances in solar-driven hygroscopic water harvesting", *Global Challenges*, 5, 2000085, 2021.
- [4] Bergmair, D., Metz, S.J., de Lange, H.C. and Steenhoven, A.A., "System analysis of membrane facilitated water generation from air humidity", *Desalination*, 339, 26-33, 2014.
- [5] Clus, O., Ortega, P., Muselli, M., Milimouk, I. and Beysens, D., "Study of dew water collection in humid tropical islands", *Journal of Hydrology*, 361, 159-171, 2008.
- [6] Lu, H., Shi, W., Guo, Y., Guan, W., Lei, C. and Yu, G., "Materials engineering for atmospheric water harvesting: Progress and perspectives", *Advanced Materials*, 34, 12, 2110079, 2022.
- [7] Hanikel, N., Prévot, M.S. and Yaghi, O.M., "MOF water harvesters", *Nat. Nanotechnol.*, 15, 348-355, 2020.
- [8] Tu, R., Hwang, Y. "Reviews of atmospheric water harvesting technologies", *Energy*, 201, 117630, 2020.
- [9] Jarimi, H., Powell, R. and Riffat, S., "Review of sustainable methods for atmospheric water harvesting", *International Journal of Low-Carbon Technologies*, 15, 253, 2020.
- [10] Zhou, X., Lu, H., Zhao, F., and Yu, G., "Atmospheric water harvesting: A review of material and structural designs", *ACS Materials Letters*, 2, 671-684, 2020.
- [11] Poredoš, P., Petelin, N., Vidrih, B., Žel, T., Ma, Q., Wang, R. and Kitanovski, A., "Condensation of water vapor from humid air inside vertical channels formed by flat plates", *iScience*, 25, 103565, 2022.
- [12] Fujii, T., *Theory of Laminar Film Condensation*. Springer-Verlag, New-York, 1991.
- [13] Nilsson, T., Vargas, W., Niklasson, G., and Granqvist, C., "Condensation of water by radiative cooling", *Renewable Energy*, 5, 310-317, 1994.
- [14] Trosseille, J., Mongruel, A., Royon, L. and Beysens, L., "Radiative cooling for dew condensation", *International Journal of Heat and Mass Transfer*, 172, 21160, 2021.
- [15] Trosseille, J., Mongruel, A., Royon, L. and Beysens, L., "Effective substrate emissivity during dew water condensation", *International Journal of Heat and Mass Transfer*, 183, 122078, 2022.
- [16] Beysens, D., Muselli, M., Milimouk, I., Ohayon, C., Berkowicz, S.M., Soyeux, E., Mileta, M. and Ortega, P., "Application of passive radiative cooling for dew condensation", *Energy*, 31, 2303-2315, 2006. ,
- [17] Tomaszkiwicz, M., Abou Najm, M., Beysens, D., Alameddine, I. and El-Fadel, M., "Dew as a sustainable non-conventional water resource: a critical review", *Environmental Reviews*, 23, 425-442, 2015.
- [18] Beysens, D., Steyer, A., Guenoun, P., Fritter, D. and Knobler, C., "How does dew form?", *Phase Transitions*, 31, 219-246, 1991.
- [19] Clus, O., Ortega, P., Muselli, M., Milimouk, I. and Beysens, D., "Study of dew water collection in humid tropical islands", *Journal of Hydrology*, 361, 159-171, 2008.

- [20] Beysens, D., Milimouk, I., Nikolayev, V., Muselli, M. and Marcillat, J., "Using radiative cooling to condense atmospheric vapor: A study to improve water yield", *J Journal of Hydrology*, 276, 1–11, 2003.
- [21] Faghri, A. and Zhang, Y., *Fundamentals of Multiphase Heat Transfer and Flow*, Springer, New-York, 2020.
- [22] Fox, R.W., McDonald, A.T., Pritchard, P.J. and Mitchell, J.W., *Introduction to Fluid Mechanics*, Wiley, China, 2014.
- [23] Bejan, A., *Convection Heat Transfer*, Wiley, New Jersey, 2013.
- [24] Chen, C.J. and Jaw, S.Y., *Fundamentals of Turbulence Modeling*, Taylor & Francis, Washington, 1997.
- [25] Bejan, A. and Kraus, A.D., *Heat Transfer Handbook*, Wiley, New Jersey, 2003.
- [26] Incropera, F.P., Dewitt, D.P., Bergman, T.L. and Lavine, A.S., *Principles of Heat and Mass Transfer*, Wiley, Singapore, 2017.
- [27] Cengel, Y.A., *Heat Transfer, A Practical Approach*, Mc Graw Hill, New York, 1997.
- [28] Chen, S.L., Gerner, F.M. and Tien, C.L., "General film condensation on plane and axisymmetric bodies in non-uniform gravity", *Journal of Heat Transfer*, 93, 97-100, 1987.
- [29] Cengel, Y.A., *Thermodynamics, An Engineering Approach*. Mc Graw Hill, New York, 2018.
- [30] Bejan, A., "Film condensation on an upward facing plate with free edges", *International Journal of Heat and Mass Transfer*, 34, 578-582, 1991.
- [31] Parkash, O., Kumar, A., and Karwar, B.S., "CFD modeling of slurry pipeline at different Prandtl numbers", *Journal of Thermal Engineering*, 7, 951-969, 2021.
- [32] Joshi, T., Parkash, O. and Krishan, G., "Slurry flow characteristics through a horizontal pipeline at different Prandtl number", *Powder Technology*, 413, 118008, 2023.